ELSEVIER

Physica A 281 (2000) 393–403

PHYSICA A

www.elsevier.com/locate/physa

Microscopic morphology and energy surface landscape in a supercooled soft-sphere system

Wen-Jong Ma[a,*], Ten-Ming Wu[b]

[a] *Institute of Mathematics, Academia Sinica, Nankang Taipei Taiwan, ROC*

[b] *Institute of Physics, National Chiao-Tung University Hsin-Chu, Taiwan, ROC*

Abstract

We carry out a systematic study on the microscopic morphology and its relationship with the signatures of the traces swept over the potential energy surface in a soft-sphere fluid system interacting via a truncated Lennard–Jones potential. The state of the model system is tuned by changing its temperature obtained in a molecular dynamics simulation, ranging from the equilibrium fluid phase to the deeply quenched supercooled states. The density and the range of interaction are chosen so that the instantaneously barely isolated centers are present. We analyze the microscopic structural origin of the features in the instantaneous-normal-mode (INM) spectrum and search for evidence of state transformation. It is found that the presence of drastic changes in the INM spectra upon entering the deep supercooled regime is accompanied by the reduction in the spatial connectivity. We develop a method to characterize the spatial configuration in an attempt to address the origin of the temperature-dependent changes in the spectra.
© 2000 Elsevier Science B.V. All rights reserved.

PACS: 63.50.+x; 61.20.ja; 61.43.Fs

Keywords: Instantaneous normal modes; Supercooled; Cluster; Percolation

1. Introduction

In the study of fluids in their liquid or glassy states, one challenging issue is the characterization of the spatially disordered configurations and its relationship to the dynamic properties of the systems. The issue becomes important as the experimental advances push to pursuit the underlying physics of the structurally originated dynamic phenomena which have been proposed as the ‘hallmarks’ for those thermodynamic

* Corresponding author. Fax: (886)02-27827432.

E-mail address: wjm@math.sinica.edu.tw (W.-J. Ma)

0378-4371/00/$ - see front matter © 2000 Elsevier Science B.V. All rights reserved.
PII: S0378-4371(00)00045-5

equilibrium or nonequilibrium states with time-varying spatial disorders. If we take the view that the dynamic signatures of an equilibrium phase or a metastable state provide the information on the evolving traces in the state space under the given macroscopic conditions, then we can employ the information to reveal the scenario of the conveyed landscape of the potential energy surface [1,2]. The systematic knowledge can be organized on the searching for the physical origins behind the various prototypes of the energy surface landscape.

Using molecular dynamics (MD) simulation as a way to sample the points along the traces in the $3N$-dimensional space of position coordinates, in an N-particle system, the curvatures at these points over the total potential energy surface defined on the $3N$-dimensional space can be obtained by performing the normal-mode calculations under a harmonic approximation. The normal mode (termed instantaneous normal mode, INM [3,4]) spectra obtained under such a scheme have been studied for simple model fluids and material systems, in their equilibrium liquid phase or undercooled states. Various types of INMs can be briefly classified according to the range of the eigen frequencies and the spatial extent involved; or may be refined further by referring to more elaborated parameters. It is the physical origin behind each type of INMs that provides the insight. It has been found that certain types of INMs can be agitated or diminished by adjusting the local property such as the shape of the interaction potential between pairs of particles [5,6], or by changing the macroscopic state in tuning the global parameters – the temperature, the density, etc. [7]. One issue raises discussions within the INM [7] or other similar context [8–10], is the presence of the quasi-localized low-frequency modes in the supercooled and glassy states. While the occurrence of these quasi-localized modes is realized as closely related to the presence of specific local arrangement, an effective characterization of the spatial configurations and its connection to the spectra in these spatially disordered systems is still not established.

In our previous studies [6], we considered a system of purely repulsively interacting particles. The interaction potential is a Lennard–Jones 6–12 potential with a cutoff distance at the minimum. In simulation, the potential is lifted by a constant value so that both the force and the potential are continuous at the cutoff. One interesting phenomena in the system is that the short interaction distance, as compared with the size of the particles, helps the formation of instantaneously barely isolated centers in the liquid state if the density is tuned properly [11]. These local centers agitate low-frequency localized modes [6,8,9] which can be related to the 'resonance modes' present in the phonon spectra of a crystalline solid contaminated by heavy impurities [12]. It is observed that density is the only important macroscopic parameter for the formation of such 'instantaneous resonance modes' (IRM) [6]. The temperature seems to have much less effect on the presence of IRMs in the equilibrium liquid states [11].[1] In this study, we consider the temperature effect in the nonequilibrium supercooled states below the liquid–solid transition point in a constant density environment. One prominent effect is

[1] In a recent study of liquid gallium by T.M. Wu and S.F. Tsay, it is found that the IRMs can also be generated by the particular nature of the interaction potential.

the absence of the energy–cost local structures in the deep supercooled regime, where the tiny kinetic energy for each individual particle prevent the particle from approaching its neighbors and only shallow contact between particles be present. Consequently, there are more particles loosing every contact with other particles instantaneously in lower temperatures. The instantaneous configuration becomes scattered with cavities that only one single isolated particle is allowed to reside in each cavity. Correspondingly, both the INM and the IRM spectra encounter, drastic qualitative changes. The main motivation of the current study is to develop effective methods characterizing these low-temperature configurations in an attempt to address the physical origin of those changes in the INM spectra.

2. MD simulations and INM spectra

We consider a system of $N=750$ particles of density $\rho = 0.88$ in a space subject to periodic boundary condition in a microcanonical (NVE) MD simulation [13]. The interaction potential is $V(r) = V_{\mathrm{LJ}}(r) + \varepsilon$, where $V_{\mathrm{LJ}}(r) = 4\varepsilon((\sigma/r)^{12} - (\sigma/r)^{6})$ with a cutoff distance $r_{\mathrm{c}} = 2^{1/6}\sigma$, the minimum of $V_{\mathrm{LJ}}(r)$. All quantities in this paper are in the reduced units derived from the length σ, the energy ε and the mass m. Starting from $T=0.192$, below which our truncated Lennard–Jones (abbreviated as TLJ) system would crystallize if the simulation time were long enough to allow for sufficient decay to equilibrium state, we decreases the temperature stepwisely [14] in intervals of $\Delta T = 0.027$. The lowest temperature reached is $T = 0.003$, about only 1.5% of the melting temperature $T_{\mathrm{m}}(\approx 0.192)$. At the beginning of each temperature change, the system is equilibrated at the desired temperature for 4τ ($\tau = \sqrt{m\sigma^2/\varepsilon}$). The system is then relaxed for the next 16τ under the NVE simulation. This finishes one stage of the preparation and the temperature is then changed to a lower value for the next stage. For each preparation stage, the system will be allowed to evolve further for an extended 40τ starting from the end of that stage. If the system is stable over this extended period, we collect the productive data over the first-half (20τ) of this period. Otherwise, the run is either abandoned if there is any evidence of crystallization, or allowed for longer preparation and data-collection periods. Indeed, the longer simulation periods are required for the two lowest temperatures ($T=0.03$ and 0.003) studied in our simulation. Since the system is in nonequilibrium state, all the results for each temperature have been examined over independent runs to guarantee consistency.

The density of states of INMs consist of two lobes, for the real and the imaginary eigen frequencies, corresponding to the positive and the negative curvatures, respectively, along their eigenvector-direction over the potential energy surface. In the equilibrium states, the main features for the real and the imaginary lobes of the spectrum include a region of extended modes over the intermediate frequency regime [6]. The region is characterized by the proportionality of the participating-particle-number R_N^{α} for a mode α to the size N of the system. Taking the square of $|\boldsymbol{e}_j^{\alpha}|$ as a measure of the statistical weight of the particle j in the mode, the number R_N^{α} is

calculated by

$$R_N^\alpha = \left(\sum_{j=1}^{N} |e_j^\alpha|^4 \right)^{-1}, \tag{1}$$

where the INM eigenvector $(e_1^\alpha, e_2^\alpha, \ldots, e_N^\alpha)$ is normalized in the $3N$-dimensional space. While the modes on the high frequency sides beyond the extended mode regimes are realized as non-extended, corresponding to highly locally strained structure [15], there are other complications in the low-frequency non-extended INMs, subject to clarification. It has been found in our TLJ system the presence of signatures of instantaneous localized resonance modes in the imaginary branch of the equilibrium liquid state, as a result of the presence of temporary barely isolated centers [6,11] (see footnote 1). In order to separate the IRM from the rest modes, a quantity s^α – the 'reduced participation ratio', defined as the ratio between Q_N^α and R_N^α, where Q_N^α is the quantity R_N^α with the contribution from the largest amplitude particle excluded [6]. A resonance mode, characterized by a large-amplitude center accompanied by the small-amplitude surroundings, would have small s [6].

Entering the supercooled regime, the spectra change smoothly with no major qualitative difference from those of equilibrium phase [6] until reaching the deep supercooled regime. Fig. 1(a) shows the density of states spectra for all INMs in the upper part ($T=0.166$, 0.138 and 0.111) and the lower part ($T=0.03$ and 0.003) of the supercooled regime. In Fig. 1(b), we consider only those INMs satisfying the criterion $s^\alpha < 0.1$. There are three isolated branches, one in the high-frequency real-mode regime (beyond the scope shown in Fig. 1(b)), the second and the third distributed on the low- and the high-frequency sides in the imaginary lobe, respectively (Fig. 1(b)). It is the low-frequency imaginary branch recognized as IRMs [6,15]. From Fig. 1, we have the following observations:

(I) the INMs in the imaginary frequency lobe, both IRMs and non-IRMs, are squeezed toward zero frequency, with the sharper distributions;
(II) the INMs in the vicinity of zero frequency in the real lobe become vanishing as temperature goes down into the deep supercooled(glassy) regime. This leads to a separation of the distribution in the real frequency lobe from that in the imaginary lobe.

3. Microscopic morphology

To characterize the changes in the spatial configurations, we first collect the information on the local arrangement of the neighbors around the particles (Figs. 2 and 3). Fig. 2(a) shows the percentage of particles considered in the simulation that having the given number of interacting neighbors at temperatures $T = 1.3, 0.83$ and 0.505 in the equilibrium fluid phase; and those for the states in the supercooled regime considered in Fig. 1. As the temperature is lowered into the supercooled regime, the

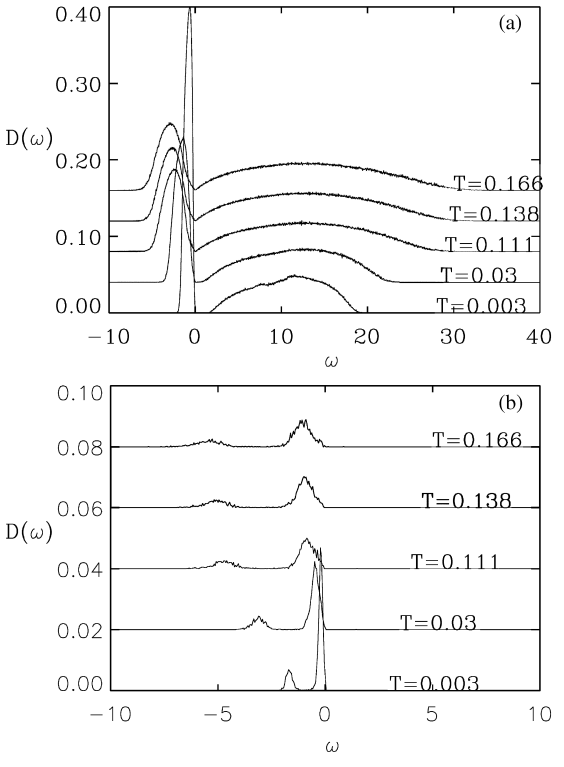

Fig. 1. (a) The densities of states of INMs in the upper part ($T = 0.166, 0.138$ and 0.111) and the lower part ($T = 0.03$ and 0.003) of the supercooled regime. (b) the densities of states satisfying the criterion $s^{\alpha} < 0.1$. There are three isolated branches satisfying this criterion. A high-frequency real-mode branch is in the regime of the high-frequency non-extended modes and is not shown in this plot. The INMs in the branch close to the zero frequency in the plot are IRMs. Note that the curves in (a) and (b) have been shifted upward in equal spacing for the better reading and the data for the δ-function-like peaks at the zero frequency have been left out.

distribution of the first layer neighbors defined by the first peak of the pair distribution function $g(r)$ (Fig. 2(b)) becomes narrow and the top of the second peak splits into two tiny subpeaks, as is typified for the supercooled liquids. The distribution of the number of interacting neighbors shift toward the low-value end (Fig. 2(a)), indicating pairs of particles loosing contact with each other. This tendency is highlighted by the sharp rising inner edge in the first peak of $g(r)$ at T=0.003 (Fig. 2(b)). Note that, at the density $\rho = 0.88$ and cutoff $r_c \approx 1.122462$, some of the first layer neighbors are beyond the interaction range with the center particle. That is, we are looking at the dense-packed configurations of spheres that parts of the neighboring contacts (defined as the first-peak-neighbor relationship in $g(r)$ with the particle at center) are not 'anchored' to contribute as a constraint on the collective motion and the number of these non interacting neighbors increases as temperature is lowered. In the following, we develop methods to characterize the global configurations. We consider each pair of interacting particles as having a 'bond' in between. We first continue the detailed

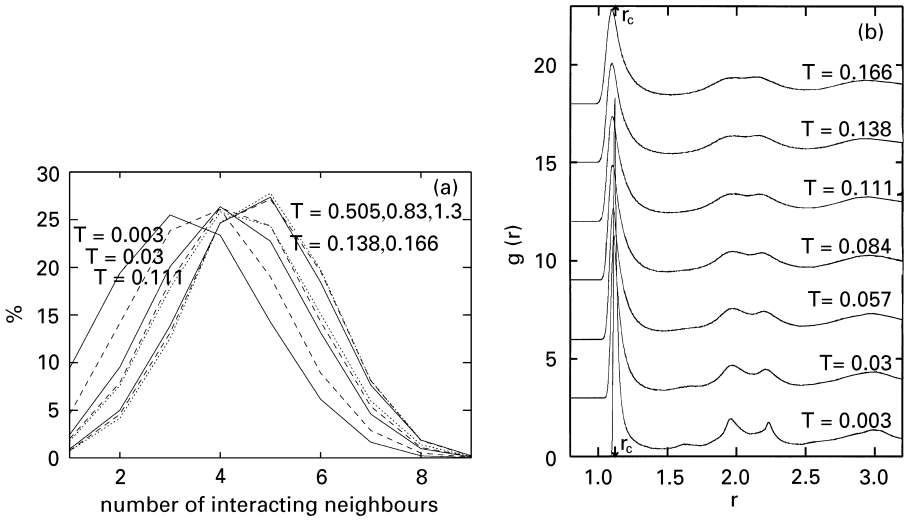

Fig. 2. (a) The percentage of particles considered in the simulation that having the given (integer) number of interacting neighbors in the equilibrium fluid phase at $T = 1.3$ (dotted line), 0.83 (dashed line) and 0.505 (solid line); in the upper supercooled regime at $T = 0.166$ (dotted line), 0.138 (dashed line) and 0.111 (solid line); and in the deep supercooled regime at $T = 0.03$ (dashed line) and 0.003 (solid line) regimes. The variation in the distribution in lowering the temperature is almost not detectable for the equilibrium phase. It becomes prominent upon entering the supercooled regime and there emerges large shifts toward the smaller values in the deep supercooled regime. (b) The pair distribution function $g(r)$ for the supercooled states. It can be seen that only parts of the first layer neighbors, defined by the first peak of $g(r)$, are beyond the interaction distance $r_c \approx 1.122462$. The curves have been shifted upward in equal spacing to make them convenient for reading.

examination on the local configuration around each particle in the major percolation cluster of each snapshot, which contains more than 97% of the particles, in the density considered in our system. We then look for the basic 'building blocks' to construct the whole cluster, based on the local information. The intention is to find any possible relationship between the geometry of packing and the effective extent of the dynamic modes.

In the INM analysis, we calculate the normal modes for each of the instantaneously 'frozen' configurations. In the following, we analyze the configurations and consider the possible constrictions on the local motion of the particles in the configuration. Consider those interacting neighbors around an arbitrarily chosen particle (a 'center'). According to our picture, there are bonds between these interacting neighbors and the center. Intuitively, we recognize that the presence of those imaginary 'bonds' constrains the motion of the center particle. Further constraint may be effective on its motion if bonds are also present in between pairs of its interacting neighbors. It seems sensible to analyze the connectivity of the configurations, in order to abstract the information on the global motion of the particles [16]. In reality, the motion depends not only on the connectivity but also on the details of the relative positions among particles. Nevertheless, such approximation should be able to provide useful information for

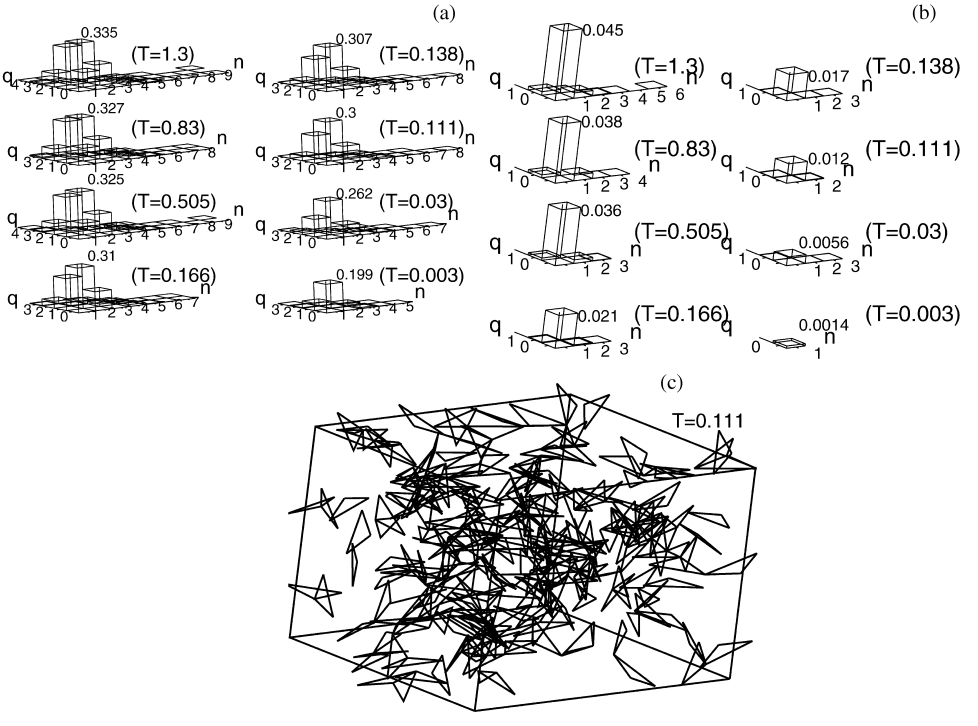

Fig. 3. (a) The fraction $f(n,q)$ of centers having $n\,q$-type bonds at each temperature, the value at the top of each subgraph labeling the highest value ($n=1, q=0$) at that temperature (b) the fraction $h(n,q)$ of centers having $n\,q$-type facets at each temperature, the value at the top of each subgraph labeling the highest value ($n=1, q=0$) at that temperature (c) the triangular facets in a typical snapshot of configuration at $T^*=0.111$. The system is in a cubic simulation box, subject to the minimum image convention [13] of the periodic boundary condition. The images out of the box for some of the particles are plotted in order to show the triangles.

our TLJ system, especially in the low temperatures, when particles have only shallow contact with one another.

In order to measure the degree of connectivity at various temperatures, we first classify the local configuration of interacting neighbors by considering two levels of structures around a particle: (a) a 'neighboring bond' connecting two of its interacting neighbors; (b) a triangular 'facet' formed by three bonds between the pairs among three interacting neighbors that interact with one another. We can classify the type of each neighboring bond according to the number of particles q, that share that bond as their neighboring bond. The local configuration around a particle can be characterized by a set of numbers n_q, the number of neighboring bonds belong to type q, for $q=0,1,2,3,\ldots$. If we count the number of particles (as centers) in the percolation cluster in all configurations sampled at a given temperature that belong to type (q,n), for each $q=0,1,2,3,\ldots$ and divide it by the total number of particles, we get a function $f(q,n)$ which gives the fraction of particles that have n type-q neighboring bonds. It characterizes the local morphology of configurations at that given temperature.

Fig. 3(a) shows $f(q,n)$ vs. q and n, in a 50-configuration sampling at each temperature. There are always some amount fraction of centers (particles) having one ($n=1$) or more ($n \geqslant 1$) neighboring bonds that are not shared ($q = 0$) or shared only by one ($q = 1$) of the other centers at all temperatures. The centers that have neighboring bond(s) shared by more than two ($q \geqslant 2$) centers are very rare, indicating a loose packing. In lowering the temperature, a major qualitative change in entering the deep supercooled regime is the drop of $f(q,n)$ for $q = 2$, suggest a further reduction in the connectivity. We can extend the calculation to the neighboring 'facets'. The function $h(q,n)$ in Fig. 3(b) gives the fraction of centers having n neighboring facets each of which is shared by other q centers as neighboring facet. There are only less than five percent centers having at least one neighboring facet ($n > 0$), let alone sharing the facet with other centers to form a tight three-dimensional structure. It is, therefore, more sensible to consider a global structure built up starting from two dimensional triangular facets [17]. Fig. 3(c) shows the plot of such triangular facets of a configuration at $T = 0.111$. We proceed to carry out the analysis on how the clusters can be constructed based on these triangular facets.

In order to construct clusters based on the triangular facets, we consider how the facets can be connected. Two triangular facets can be connected neither by a bond, nor by sharing one or two particles. We classify the clusters (of triangular facets) formed by any of the three kinds of connection as type A clusters. The clusters connected only by sharing particle(s) are called type B. Fig. 4(a) shows that the average number of type A clusters can be found over a 50-configuration sampling. In Fig. 4(b), the data counts only those type A clusters that percolate. Lowering temperature reduces the sizes of the type A clusters most of which are percolation clusters with the exception in the deep supercooled states ($T = 0.03$ and 0.003). In the later cases, many small clusters are localized (compare Fig. 4(a) and (b)). The data of all clusters and of percolation clusters of type B are shown in Fig. 5(a) and (b), respectively. In the equilibrium liquid regime well above the melting point (see $T = 1.3$ and 0.83 in Fig. 5(a)), there are two subgroups of type B clusters distributed separately according to sizes. Almost all of the clusters in the larger-size subgroup are percolation clusters as can be seen in Fig. 5(b). Lowering temperature, this subgroup start to merge with the smaller-size one and correspondingly lose the percolation property. At $T = 0.03$ and 0.003, there are no any percolation clusters of type B at all. We summarize that the general behavior of type A clusters in lowering the temperature is the evolving from larger and extended (percolation) clusters to smaller and localized (non-percolation) ones. For each configuration, there is always one single dominated type A cluster, which looses its integrity only in the deep supercooled regime as small pieces separate away. For type B clusters, on the other hand, the extended and localized clusters alway coexist in each configuration. They can be distinguished according to their sizes if the system is in the high-temperature equilibrium liquid regime. Lowering temperature smears such division and the clusters become completely localized in entering the deep supercooled regime.

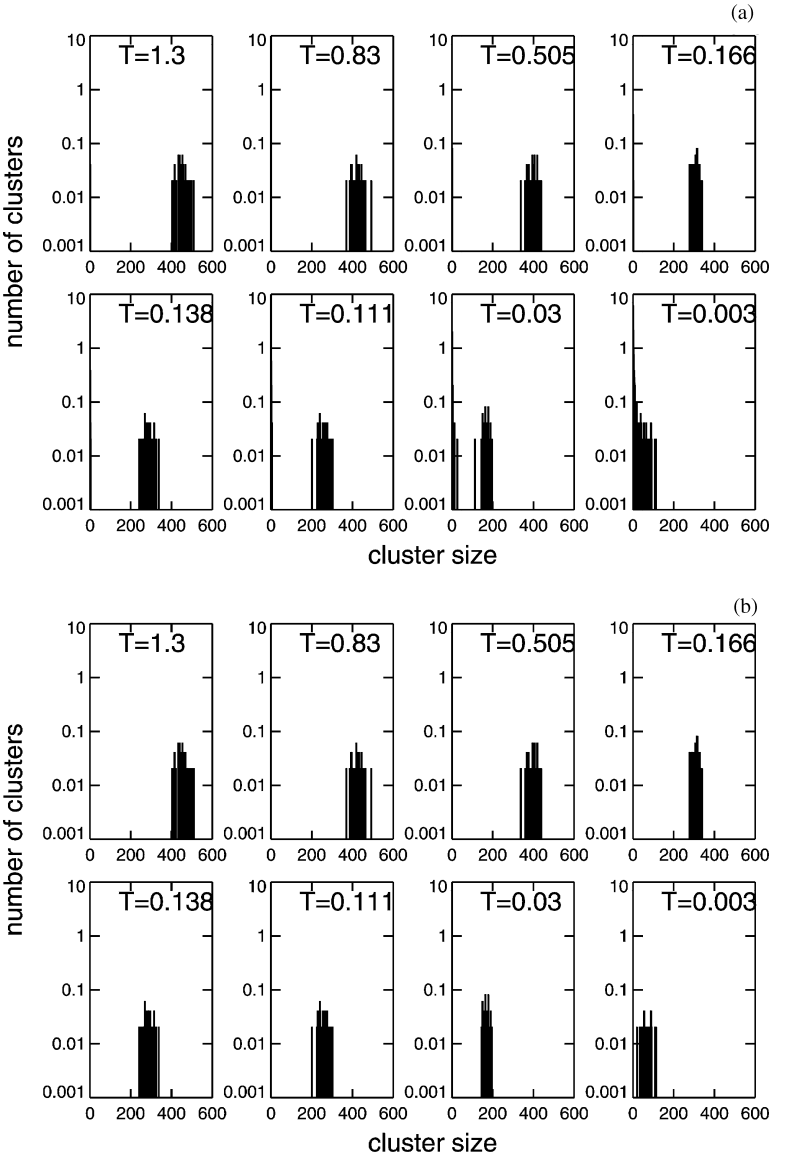

Fig. 4. (a) The averaged number of type A clusters can be found over a 50-configuration sampling. In (b), the data counts only those type A clusters that percolate. In a comparsion between (a) and (b), it found that virtually all type A clusters are percolation clusters at temperatures, ranging from the equilibrium phase ($T = 1.3, 0.83, 0.505$), to the upper supercooled regime ($T = 0.166, 0.138, 0.111$). Lowering the temperature reduces the sizes of these clusters. In entering the deep supercooled regime ($T = 0.03, 0.003$), some small clusters become nonpercolating. (Note the vertical axes are in logarithmic scales.)

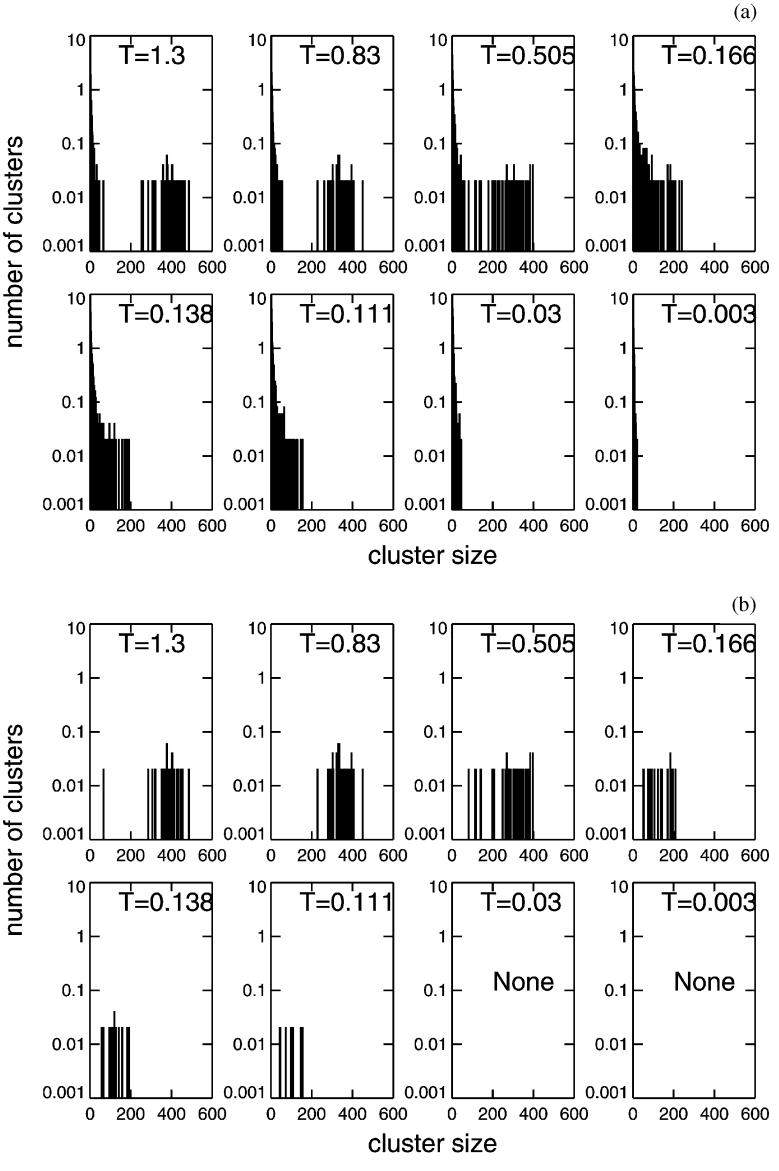

Fig. 5. (a) The averaged number of type B clusters can be found over a 50-configuration sampling. In (b), the data counts only those type B clusters that percolate. The percolation and nonpercolation type B clusters are well separated according to their sizes at high temperatures ($T = 1.3, 0.83$). Such division become smeared as temperature goes down. In the deep supercooled regime, all type B clusters do not percolate. (Note that the vertical axes are in logarithmic scales.)

4. Discussion

How would the observations (I) and (II) on the INM spectra mentioned above be related to the structural information discussed so far? For observation (I), in the

deep supercooled regime, the reduction in the number of interacting neighbors and the shallow contact between a particle and its interacting neighbors leads to the smaller curvatures over the potential surface and, correspondingly, smaller frequencies. A better understanding of whether there is a direct or indirect correlation between the diminishing of near-zero frequency real modes (observation (II)) and the crossovers in structure requires, on the other hand, further studies on the physical nature of the clusters [16,18].

Is there any evidence of state transformation? The analysis of diffusion constant and the structural changes suggest the presence of a crossover from the upper supercooled regime to the lower one, which seems consistent with the qualitative alternation signaled by the percolation properties. Since the landscape of the potential energy surface determined by the imaginary frequency INM spectra is related to the diffusion behavior in the fluid states, a better understanding of the relationship between the cluster properties discussed above and the spectra will help to answer the question.

In summary, we have developed a method to characterize the spatial configurations of the supercooled states in our TLJ soft sphere systems. The connectivity of the configurations has been analyzed by piling up triangular facets. There seems related changes in the percolation property of the clusters formed by these triangular facets and, in the INM spectra, including the diminishing of a section of the real frequency modes next to the zero frequency. Further study on the physical nature of the clusters and its relevance to the INMs is required to clarify the issue.

Acknowledgements

W.J. Ma would like to thank Prof. C.K. Hu for his guidance to the interesting problem of continuum percolation. T.M. Wu would like to acknowledge support from National Science Council of Taiwan, ROC under grant NSC 892112-M009009.

References

[1] F.H. Stillinger, T.A. Weber, Science 267 (1995) 1935.
[2] A.C. Angell, Science 267 (1995) 1924.
[3] R.M. Stratt, Acc. Chem. Res. 28 (1995) 201.
[4] T. Keyes, J. Phys. Chem. 101 (1997) 2921.
[5] T.M. Wu, W.J. Ma, S.F. Tsay, Physica A 254 (1998) 257.
[6] T.M. Wu, W.J. Ma, J. Chem. Phys. 110 (1999) 447.
[7] T.M. Wu, S.F. Tsay, Phys. Rev. B 58 (1998) 27.
[8] S.D. Bembenek, B.B. Laird, Phys. Rev. Lett. 74 (1995) 936.
[9] B.B. Laird, H.R. Schober, Phys. Rev. Lett. 66 (1991) 636.
[10] H.R. Schober, C. Oligschleger, Phys. Rev. B 53 (1996) 11 469.
[11] T.M. Wu, W.J. Ma, S.L. Chang, to be published.
[12] A.A. Maradudin, in: Localized Excitation in Solids, Plenum, New York, 1968.
[13] M.P. Allen, D.J. Tildesley, Computer Simulation of Liquids, Clarendon, Oxford, 1987.
[14] W.J. Ma, S.K. Lai, Physica B 233 (1997) 221.
[15] T.M. Wu, W.J. Ma, unpublished.
[16] D.J. Jacobs, M.F. Thorpe, Phys. Rev. E 53 (1996) 3682.
[17] F.C. Frank, J.S. Kasper, Acta Crystallogr. 11 (1958) 148.
[18] J.E. Adams, R.M. Stratt, J. Chem. Phys. 93 (1990) 1332.